((please add journal code and manuscript number, e.g., DOI: 10.1002/ppap.201100001))
Article type: Full paper

Optimization of CO_2 conversion in a cylindrical dielectric barrier discharge reactor using design of experiments

Danhua Mei, Ya-Ling He, Shiyun Liu, Joseph Yan, Xin Tu*

———

D. H. Mei, Prof. Y. L. He
Key Laboratory of Thermo-Fluid Science and Engineering, Ministry of Education, School of Energy and Power Engineering, Xi'an Jiaotong University, Xi'an 710049, China

D. H. Mei, S. Y. Liu, Dr. J. D. Yan, Dr. X. Tu
Department of Electrical Engineering and Electronics, University of Liverpool, Brownlow Hill, Liverpool, L69 3GJ, UK
E-mail: xin.tu@liverpool.ac.uk

Corresponding author

Dr. Xin Tu

Department of Electrical Engineering and Electronics

University of Liverpool

Liverpool L69 3GJ

UK

E-mail: xin.tu@liverpool.ac.uk

Abstract

In this work, a coaxial dielectric barrier discharge reactor has been developed for the decomposition of CO_2 at atmospheric pressure. The response surface methodology based on a three-factor, three-level Box-Behnken design has been developed to investigate the effects of key independent process parameters (discharge power, feed flow rate and discharge length) and their interactions on the reaction performance in terms of CO_2 conversion and the energy efficiency of the plasma process. Two quadratic polynomial regression models have been established to understand the relationships between the plasma process parameters and the performance of the CO_2 conversion process. The results indicate that the discharge power is the most important factor affecting CO_2 conversion, while the feed flow rate has the most significant impact on the energy efficiency of the process. The interactions between different plasma process parameters have a very weak effect on the conversion of CO_2. However, the interactions of the discharge length with either discharge power or gas flow rate have a significant effect on the energy efficiency of the plasma process. The optimal process performance - CO_2 conversion (14.3%) and energy efficiency (8.0%) for the plasma CO_2 conversion process is achieved at a discharge power of 15.8 W, a feed flow rate of 41.9 $ml \cdot min^{-1}$ and a discharge length of 150 mm as the highest global desirability of 0.816 is obtained at these conditions. The reproducibility of the experimental results successfully demonstrates the feasibility and reliability of the design of experiments approach for the optimization of the plasma CO_2 conversion process.

Graphic for the abstract

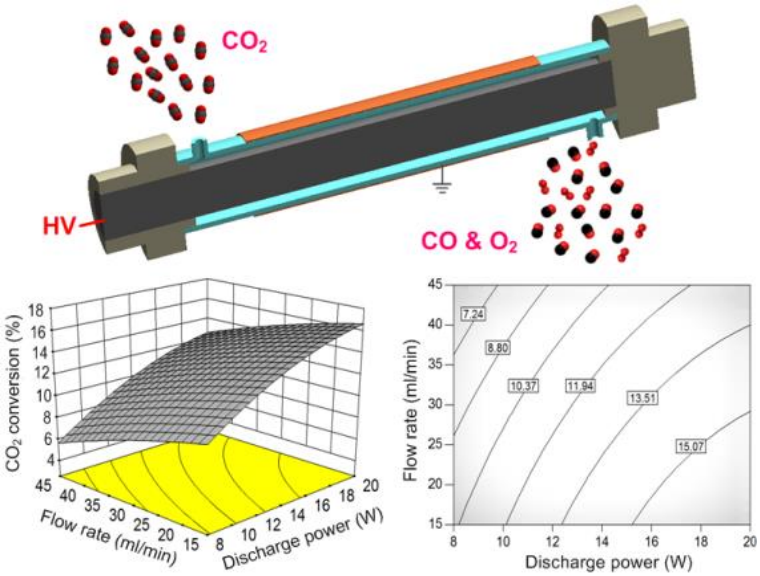

1. Introduction

The increasing energy demand of the growing population has led to the rapid consumption of fossil fuels, inevitably releasing carbon dioxide (CO_2) which is a prime contributor to global warming and climate change. For instance, the UK emits more than 470 million tons of CO_2 per year and of this 39 % is emitted by the energy and chemistry sectors.[1] The UK government has committed to reduce greenhouse gas emissions by at least 80% (from the 1990 baseline) by 2050.[2] Significant efforts have been devoted to develop innovative and cost-effective technologies to deal with the global challenge of CO_2 emissions. One promising solution is to use wasteful CO_2 emissions as feedstock for the production of value-added fuels and chemicals (e.g. CO, CH_4 and methanol). For instance, direct conversion of CO_2 into CO is an interesting chemical process, as CO is a useful chemical feedstock and can be used as a reactant to produce higher energy products such as hydrocarbons and liquid fuels. This will ultimately not only make full use of CO_2, but will also minimize the negative environment impacts due to carbon emissions. However, it is very challenging to convert CO_2 in an energy-efficient and cost-effective way due to the high stability of CO_2 molecules. A large amount of energy is required for thermal or catalytic decomposition of CO_2 into CO as it is an endothermic reaction due to the positive reaction enthalpy change ΔH as shown in Equation 1.

$$CO_2 \rightarrow CO + \frac{1}{2}O_2 \qquad \Delta H = 280\ \mathrm{kJ \cdot mol^{-1}} \tag{1}$$

Extensive efforts have been made to convert CO_2 with or without hydrogen into higher value fuels and chemicals using photochemical and electrochemical catalytic reactions.[3, 4] Despite their great potential, significant fundamental work is still required to further improve the overall energy efficiency and product selectivity of the processes by developing new reactor systems and novel catalytic materials with higher reactivity and stability, especially the generation of cost-effective renewable hydrogen.

Non-thermal plasma technology has been regarded as a promising alternative to the thermal catalytic route for converting low value and inert carbon emissions, such as CH_4 and CO_2, into value-added fuels and chemicals at atmospheric pressure due to its non-equilibrium characteristic, low energy cost and unique capability to induce both physical and chemical reactions at ambient conditions.[5-7] In non-thermal plasmas, the overall plasma gas temperature can be as low as room temperature, while the electrons are highly energetic with an average electron energy of 1-10 eV which can easily break down most chemical bonds of inert molecules and produce chemically reactive species such as radicals, excited atoms, molecules and ions for chemical reactions. The non-equilibrium character of such plasmas could enable thermodynamically unfavourable reactions (e.g. CO_2 splitting) to occur at low temperatures (e.g. <200 ^oC). Up to now, different plasma sources have been used for CO_2 conversion, including dielectric barrier discharge (DBD),[8-16] corona discharge,[17-19] glow discharge,[20, 21] microwave discharge,[22-24] radio frequency discharge,[25, 26] and gliding arc discharge.[27, 28] However, previous works mainly focused on the plasma conversion of CO_2 diluted with high volumes of inert gases such as helium and argon,[11, 29, 30] which are not favourable for industry applications due to the cost of these gases, especially helium, while direct conversion of pure CO_2 into value-added chemicals could be valuable if integrated with carbon capture or bio-oil upgrading processes. Plasma conversion of CO_2 is a complex and challenging process involving a large number of physical and chemical reactions. The reaction performance (CO_2 conversion and energy efficiency) of the process is totally controlled by a wide range of plasma process parameters such as the discharge power, gas flow rate, gas residence time, reactor configuration and frequency.[31] It is often of primary interest to explore the relationships between these key independent input variables and the output performance characteristics of the plasma process.

Standard experiments are designed to look at one of these parameters in isolation from the others and so screening a large number of process parameters is time-consuming and costly

due to large numbers of experiments which need to be performed. This type of experimentation requires large quantities of resources to obtain a limited amount of information about the process. A fundamental understanding of the importance of different process parameters, especially the combined effects of these parameters on the performance of plasma processing of CO_2, is very limited and not clear, which makes it difficult to determine the set of operating parameters that will optimize and maximize the performance of the plasma process. Plasma chemical modelling offers an alternative route for solving this problem. De Bie et al. developed a one-dimensional (1D) fluid model to investigate the effect of different plasma process conditions on the plasma decomposition of CH_4 in a DBD reactor.[32] The model consisted of 36 species (electrons, atoms, ions, molecules) and 367 gas phase reactions. This model was recently extended to simulate plasma methane conversion in CH_4/CO_2 and CH_4/O_2 mixtures.[33] Snoeckx et al. developed a zero-dimensional (0D) kinetics model to understand the influence of different operating parameters (gas mixture ratio, discharge power, residence time and frequency) on the conversion and energy efficiency of plasma dry reforming of CO_2 and CH_4 in a similar DBD reactor, and to investigate which of these parameters lead to the most promising results.[31, 34] However, although model calculations can be fast, depending on the type of model, the development of a comprehensive model takes time and is thus not always useful for fast and cost-effective optimization of highly complex plasma chemical processes.

Design of experiments (DoE) is a powerful tool for process optimization since it allows multiple input factors to be manipulated, determining their individual and combined effects on the process performance in the form of one or more output responses, whilst significantly reducing the number of experiments compared to conventional experiments with one factor at a time.[35] Response surface methodology (RSM) is one of the most useful experimental designing methodologies for building the relationship between the multiple input parameters and output responses, which enable us to get a better understanding of the effect of individual

158 factors and their interactions on the responses by three-dimensional and contour
159 interpretations. Two design approaches, central composite design (CCD) and Box-Behnken
160 design (BBD), have been commonly used in response surface methodology.[36] It has been
161 demonstrated that BBD is more efficient than CCD for a three-factor and three-level design
162 since fewer experiments are required using the BBD approach.[37, 38] Until now, there has been
163 only very limited work focussing on the optimization of plasma processing of materials using
164 the DoE method,[37, 39] while the use of DoE for quick optimization of plasma chemical
165 reactions, such as CO_2 conversion and utilization, has not been done before.

166 In this study, a coaxial DBD reactor has been developed for the conversion of pure CO_2
167 into CO and O_2 at atmospheric pressure. Response surface methodology based on Box-
168 Behnken design has been used to establish the relationship between the key plasma process
169 parameters and the process performance, and to optimize the performance of the plasma
170 processing of CO_2 in terms of CO_2 conversion and energy efficiency. Moreover, the influence
171 of different process parameters and their interactions on the reaction performance has been
172 investigated and discussed.

173

174 2. Experimental

175 2.1 Experimental setup

176 The experiment was carried out in a coaxial DBD reactor, as shown in Figure 1. An
177 aluminium foil wrapped around the outside of a quartz tube, with an external diameter of 22
178 mm and an inner diameter of 19 mm, acted as a ground electrode. A stainless steel rod with an
179 outer diameter of 14 mm was placed in the centre of the quartz tube and used as a high
180 voltage electrode. The length of the discharge region could be varied from 90 to 150 mm with
181 a discharge gap fixed at 2.5 mm. Pure CO_2 was used as the feed gas with a gas flow rate of
182 15-45 $ml \cdot min^{-1}$. The DBD reactor was supplied by a high voltage AC power supply with a
183 peak-to-peak voltage of 10 kV and a frequency of 50 Hz. The applied voltage was measured

by a high voltage probe (Testec, HVP-15HF), whilst the current was recorded by a current monitor (Bergoz CT-E0.5). The voltage across the external capacitor (0.47 μF) was measured to determine the charge passing through the DBD. All the electrical signals were sampled by a four-channel digital oscilloscope (TDS2014). The *Q-U* Lissajous method was used to calculate the discharge power (*P*) of the DBD reactor. A homemade online power measurement system was used to monitor and control the discharge power in real time.

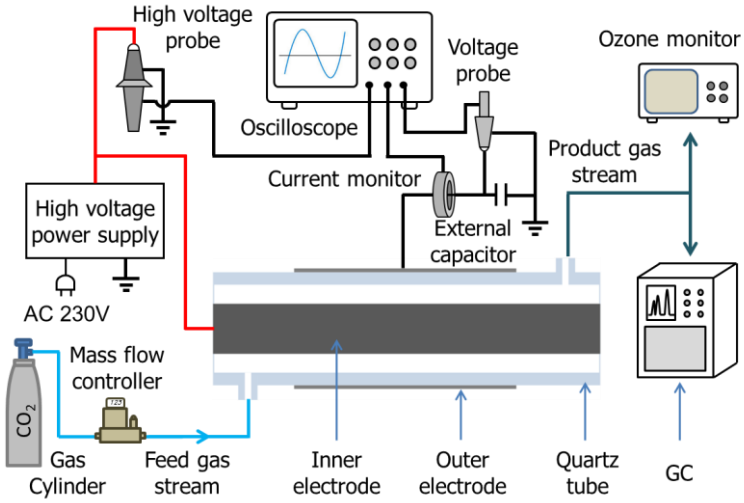

Figure 1. Schematic diagram of the experimental setup.

2.2 Product Analysis

The reactant and gas products were analyzed by a gas chromatograph (Shimadzu GC-2014) equipped with a flame ionization detector (FID) and a thermal conductivity detector (TCD). The concentration of ozone was measured by an ozone monitor (2B, Model 106-M). However, no ozone was detected in the effluent in this study. Each measurement was repeated three times and had a high reproducibility with a measurement error of less than 5%. The conversion of CO_2 (*C*), the selectivity towards CO (*S*) and the carbon balance (*B*) are defined as follows:

$$C_{CO_2}(\%) = \frac{CO_2 \text{ converted } (\text{mol}\cdot\text{s}^{-1})}{CO_2 \text{ introduced } (\text{mol}\cdot\text{s}^{-1})} \times 100 \quad (2)$$

$$S_{CO}(\%) = \frac{\text{CO produced}\left(\text{mol}\cdot\text{s}^{-1}\right)}{\text{CO}_2\text{ converted}\left(\text{mol}\cdot\text{s}^{-1}\right)} \times 100 \quad (3)$$

$$B_{\text{Carbon}}(\%) = \frac{[\text{CO}_2]_{\text{out}} + [\text{CO}]_{\text{out}}}{[\text{CO}_2]_{\text{in}}} \times 100 \quad (4)$$

The energy efficiency (E) and the specific energy density (SED) are determined from

$$E\left(\text{mmol}\cdot\text{J}^{-1}\right) = \frac{\text{CO}_2\text{ converted}\left(\text{mol}\cdot\text{s}^{-1}\right)}{\text{Discharge power}\left(\text{kW}\right)} \quad (5)$$

$$E(\%) = \frac{\text{CO}_2\text{ converted}\left(\text{mol}\cdot\text{s}^{-1}\right)\cdot \Delta H\left(\text{kJ}\cdot\text{mol}^{-1}\right)}{\text{Discharge power}\left(\text{kW}\right)} \times 100 \quad (6)$$

$$\text{SED}\left(\text{kJ}\cdot\text{l}^{-1}\right) = \frac{\text{Discharge power (W)}}{\text{CO}_2\text{ flow rate}\ (\text{ml}\cdot\text{s}^{-1})} \quad (7)$$

where ΔH is the reaction enthalpy for CO_2 decomposition (shown in Equation 1).

2.3 Surface response method

In this study, a three-factor, three-level Box-Behnken design is used to investigate the effects of each independent factor and the interactions of these factors on the reaction performance of the plasma CO_2 conversion process. Based on the results from our previous works and other papers,[9, 40] discharge power (X_1), feed flow rate (X_2), and discharge length (X_3) have been identified as the three most important independent parameters affecting plasma CO_2 conversion and thus are chosen as the inputs for the design, while CO_2 conversion (Y_1) and the energy efficiency of the process (Y_2) are identified as the responses. Each independent process parameter contains three different levels, which are coded as –1 (low), 0 (centre) and +1 (high), as shown in Table 1.

Table 1. Levels and ranges of independent input variables in the Box-Behnken design

Independent variables	Symbols	Level and range

		Low (–1)	Centre (0)	High (+1)
Discharge power (W)	X_1	8	14	20
Feed flow rate (ml·min^{-1})	X_2	15	30	45
Discharge length (mm)	X_3	90	120	150

In the BBD design, a regression model is developed to describe the relationship between a set of the input plasma process parameters and each response. The regression model can be defined as:

$$Y = \beta_0 + \sum_{i=1}^{3} \beta_i X_i + \sum_{i=1}^{3} \beta_{ii} X_{ii}^{\ 2} + \sum_{i=1}^{2} \sum_{j=i+1}^{3} \beta_{ij} X_i X_j \quad (8)$$

where Y is the response, β_0 is a constant coefficient, β_i and β_{ii} are linear and quadratic coefficients for the terms X_i and X_{ii}, respectively. β_{ij} are the coefficients which represent the interactions of X_i and X_j. This model can be used to predict the reaction performance under different process conditions.

The analysis of variance (ANOVA) is used to evaluate the adequacy and fitness of the models. The statistical significance of the models and each term in the models can be identified by the F-test and adequacy measures such as the coefficient of determination R^2, adjusted R^2 and predicted R^2. The difference between the predicted R^2 and adjusted R^2 should be within 0.2 for a well-developed model.[35]

3. Results and Discussion

In this experiment, CO and O_2 are the two gas products from plasma conversion of pure CO_2. No ozone was detected in the effluent and no carbon deposition was observed in the plasma reaction, which results in a high carbon balance (97.5%-98.2%). The selectivity of CO was within the range of 91.5%-96.1%, while the molar ratio of CO/O_2 was around 2:1. Therefore, this paper is mainly focused on the investigation of the effect of different processing

parameters on CO_2 conversion and energy efficiency and the optimization of these parameters to provide valuable information for the development of a cost-effective plasma process for CO_2 conversion.

3.1 DoE analysis

In this study, the total number of the experimental samples required for the BBD design is 18, including five replicated experimental runs using the processing parameters at the centre points (Table 2). This number is less than that required for a full factorial design (3^3=27). Quadratic models are designed to describe the relationships between the key input process parameters (factors) and the output reaction performance (i.e., CO_2 conversion and energy efficiency), as shown in Equation 9 and 10.

Table 2. Actual response of CO_2 conversion and energy efficiency at experimental design points

Exp. order	Independent input variables (X)			Response (Y)	
	X_1: discharge power (W)	X_2: feed flow rate (ml·min^{-1})	X_3: discharge length (mm)	Y_1: CO_2 conversion (%)	Y_2: Energy efficiency (mmol·kJ^{-1})
1	14	30	120	13.0	0.208
2[a)]	14	30	120	12.9	0.205
3	14	15	150	17.3	0.138
4	8	45	120	6.3	0.261
5	8	30	90	5.3	0.147
6[b)]	14	30	120	13.2	0.210
7	20	30	90	13.5	0.150
8	8	30	150	10.5	0.293
9	14	45	150	13.0	0.310
10	20	15	120	16.1	0.090

11	20	30	150	17.3	0.193
12	20	45	120	12.5	0.209
13[c)]	14	30	120	12.8	0.204
14	14	45	90	7.2	0.171
15[d)]	14	30	120	12.2	0.194
16	14	15	90	12.1	0.100
17[e)]	14	30	120	11.9	0.190
18	8	15	120	10.4	0.144

257 a)-e) Replicated experimental runs (Run order: 2, 6, 13, 15 and 17).

258
$$\begin{aligned} Y_1:\ &\mathrm{CO_2\ conversion}(\%) \\ &= -8.846 + 1.584\times X_1 - 0.125\times X_2 + 0.092\times X_3 + 1.575\times10^{-3}\times X_1X_2 \\ &\quad - 2.078\times10^{-3}\times X_1X_3 + 3.778\times10^{-4}\times X_2X_3 - 0.029\times X_1^{\,2} - 1.398\times10^{-3}\times X_2^{\,2} \\ &\quad + 3.625\times10^{-5}\times X_3^{\,2} \end{aligned} \tag{9}$$

259
$$\begin{aligned} Y_2:\ &\mathrm{Energy\ efficiency}\left(\mathrm{mmol\cdot kJ^{-1}}\right) \\ &= -0.207 + 0.017\times X_1 + 2.758\times10^{-3}\times X_2 + 2.156\times10^{-3}\times X_3 \\ &\quad + 5.556\times10^{-6}\times X_1X_2 - 1.431\times10^{-4}\times X_1X_3 + 5.611\times10^{-5}\times X_2X_3 \\ &\quad - 1.366\times10^{-4}\times X_1^{\,2} - 9.296\times10^{-5}\times X_2^{\,2} - 1.296\times10^{-6}\times X_3^{\,2} \end{aligned} \tag{10}$$

260 The ANOVA analysis is performed to determine the significance and adequacy of the
261 regression models (Table 3 and 4). The *F*-value for the regression model of CO_2 conversion
262 and energy efficiency is 50.65 and 145.08, respectively, both of which are higher than the
263 critical value (3.39 in our case),[35] which suggests that both models are statistically significant
264 and represent the correlation between the input process parameters and the performance of the
265 plasma process. This can also be evidenced by a good agreement (R^2 close to 1) between the
266 experimental data and the simulated values from the regression models, as shown in Figure 2.
267 In addition, for both CO_2 conversion and energy efficiency, the values of the predicted R^2 are
268 in agreement with those of the adjusted R^2 (the difference between the predicted R^2 and
269 adjusted R^2 is less than 0.2 for each response), which also demonstrates the stability and

validity of the models. These results show that both regression models are statistically significant and adequate for the prediction and optimization of the plasma CO_2 conversion process.

Table 3. Results of ANOVA for the quadratic model of the conversion rate of CO_2

Model terms	Sum of square	DF[a)]	Mean square	*F*-value	*p*-value (Prob>*F*)
Model	182.41	9	20.27	50.65	<0.001
X_1	90.51	1	90.51	226.20	<0.001
X_2	35.98	1	35.98	89.93	<0.001
X_3	49.50	1	49.50	123.71	<0.001
X_1X_2	0.080	1	0.080	0.20	0.6659
X_1X_3	0.56	1	0.56	1.10	0.2710
X_2X_3	0.12	1	0.12	0.29	0.6056
X_1^2	4.86	1	4.86	12.15	0.0082
X_2^2	0.43	1	0.43	1.08	0.3292
X_3^2	4.645E-3	1	4.645E-3	0.012	0.9169
Residual	3.20	8	0.40		
Total	185.61	17			

R^2: 0.9828; adjusted R^2: 0.9634; predicted R^2: 0.9215

a) degree of freedom.

Table 4. Results of ANOVA for the quadratic model of the energy efficiency

Model terms	Sum of square	DF[a)]	Mean square	*F*-value	*p*-value (Prob>*F*)
Model	0.058	9	6.439E-3	145.08	<0.001

X_1	5.151E-003	1	5.151E-3	116.05	<0.001
X_2	0.029	1	0.029	646.16	<0.001
X_3	0.017	1	0.017	377.25	<0.001
X_1X_2	1.000E-6	1	1.000E-6	0.023	0.8844
X_1X_3	2.652E-3	1	2.652E-3	59.75	<0.001
X_2X_3	2.550E-3	1	2.550E-3	57.46	<0.001
X_1^2	1.055E-4	1	1.055E-4	2.38	0.1617
X_2^2	1.909E-3	1	1.909E-3	43.01	0.0002
X_3^2	5.939E-6	1	5.939E-6	0.13	0.7240
Residual	3.551E-4	8	4.439E-5		
Total	0.058	17			

R^2: 0.9939; adjusted R^2: 0.9871; predicted R^2: 0.9827

a) degree of freedom.

278

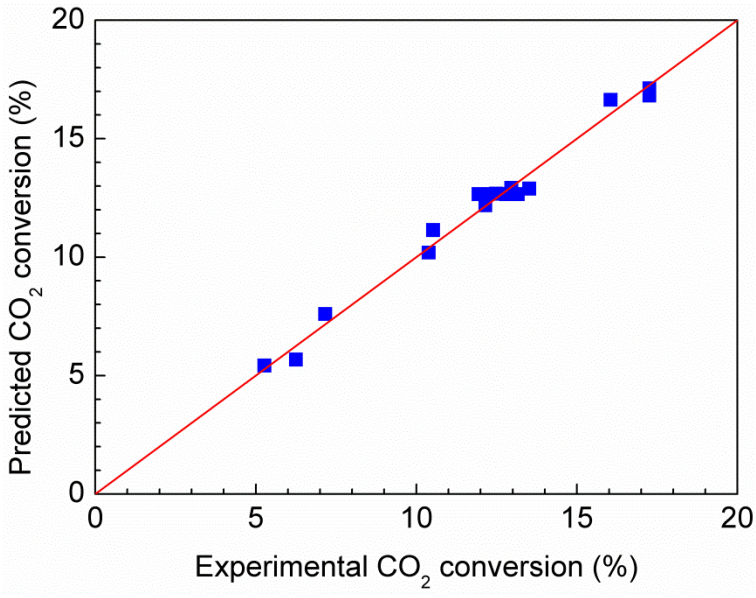

279

280 (a)

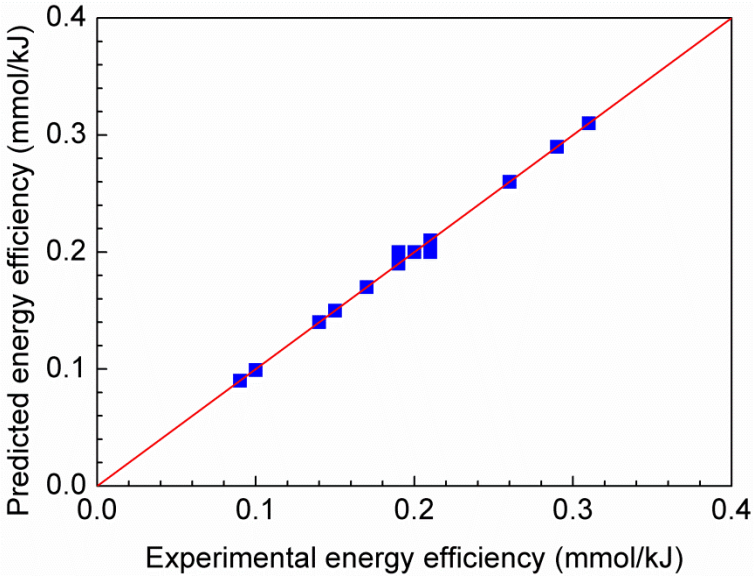

(b)

Figure 2. Comparison of experimental and predicted results (a): CO_2 conversion; (b) energy efficiency.

3.2 Effect of plasma process parameters on CO_2 conversion

If the *p*-value of a term (individual factor X_i or interaction of two factors X_iX_j) is below the critical value of 0.05 (level of significance), the corresponding term is considered to have a significant impact on the process performance. In the plasma CO_2 conversion, X_1, X_2, X_3, and X_1^2 are identified as the significant terms, while the terms X_1X_2, X_1X_3, X_2X_3, X_2^2, and X_3^2 play a weak role in the reaction, which suggests that the individual plasma process factor is considered to be more important than the interactions between different factors in terms of CO_2 conversion. The relative importance of a term is determined by its *F*-value. The discharge power has the most significant impact on CO_2 conversion compared to the other factors due to its highest *F*-value of 226.20 (shown in Table 3).

The effects of different process parameters and their interactions on CO_2 conversion are presented in the form of a three dimensional response surface and projected contour derived from the regression equation (Equation 9), as shown in Figure 3-5. If there is no or weak interaction between two process parameters, the fitted response surface will be a plane (i.e.

contour lines will be straight). In contrast, if two different process parameters strongly interact, the contour lines will be curved rather than straight, while the contour produced by a second-order model will be elliptical. This phenomenon can also be reflected from the gradient of the response (e.g. CO_2 conversion and energy efficiency) with respect to one of these process parameters. If two process parameters have a significant interaction effect, the gradient of the response to one process parameter can be significantly different when changing the other parameter.

Figure 3 shows the effects of the discharge power and reactant flow rate on CO_2 conversion at a discharge length of 120 mm. A maximum CO_2 conversion of 16.1% is achieved at the highest discharge power (20 W) and lowest CO_2 flow rate (15 ml·min^{-1}). The conversion of CO_2 increases with the increase of the discharge power from 8 W to 20 W, regardless of the changes in gas flow rate, which can be reflected by a nearly constant gradient of CO_2 conversion with respect to the discharge power (0.48% W^{-1} at the gas flow rate of 15 ml·min^{-1} and 0.52% W^{-1} at the flow rate of 45 ml·min^{-1}), as plotted in Fig. 3(b). This suggests that the effect of the interaction between the discharge power and CO_2 flow rate on CO_2 conversion is insignificant. This can also be confirmed by the high *p*-value (0.6659) of the term X_1X_2.

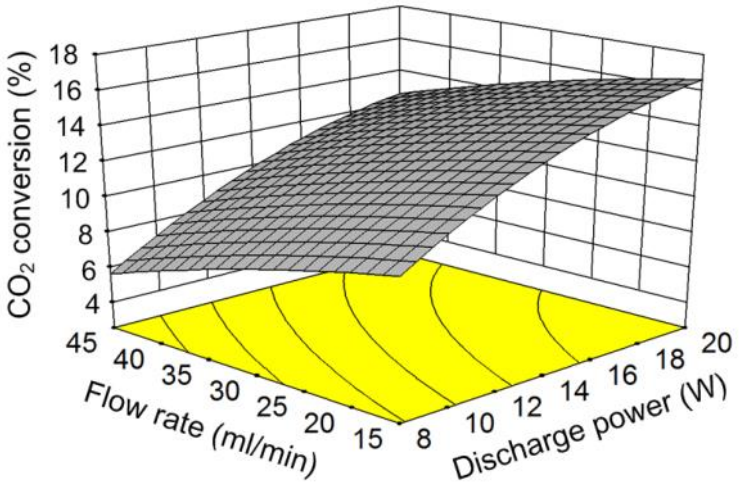

(a)

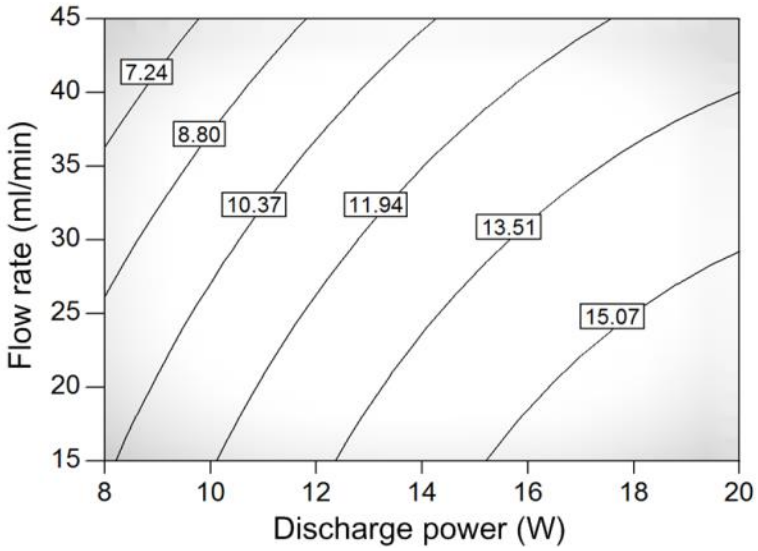

(b)

Figure 3. Effect of discharge power, feed flow rate and their interaction on CO_2 conversion at a discharge length of 120 mm (a) 3D surface plot; (b) projected contour plot.

In this study, the CO_2 DBD can be characterized as a typical filamentary discharge. The discharge power is changed by adjusting the applied voltage at a fixed frequency. Increasing the discharge power by only changing the applied voltage does not change the average electric field of the plasma since the gas voltage and breakdown voltage of the CO_2 DBD is almost constant (calculated from the Lissajous figure [7]), with the increase of the discharge power. This also means that the average electron energy in the CO_2 discharge does not change when changing the discharge power at a constant frequency, which can be shown from Einstein's equation.[41] In contrast, we find that the number of microdischarges and the current intensity in the CO_2 DBD increase with the increase of the discharge power or applied voltage, which can be observed from the increased number and amplitude of the current pulses in the electrical signals. Dong et al also reported that the number of filaments per unit dielectric surface in a DBD reactor increases with the increase of the applied voltage.[42] The increased number of microdischarges in the CO_2 DBD suggests the formation of more reaction channels

and electrons in the plasma, both of which contribute to the enhancement of the reaction performance (e.g. CO_2 conversion) when increasing the discharge power of the CO_2 DBD.

It was reported that CO_2 dissociation by electron impact vibrational excitation (Equation 13 and 14) is the most effective pathway for CO_2 conversion in non-thermal plasmas and that up to 97% of the plasma energy can be transferred from electrons to vibrational excitation of CO_2 at an electron temperature of 1-2 eV, or a reduced electric field (E/N) of 20-40 Td.[43]

$$e + CO_2 \rightarrow e + CO_2(\upsilon^*) \quad (11)$$

$$e + CO_2(\upsilon^*) \rightarrow e + CO + O \quad (12)$$

Here v^* is the vibrational excited state. However, Aerts et al developed a chemical kinetics model to understand the plasma chemistry and role of electron vibrational excitation in the CO_2 conversion in a DBD reactor with an average electron temperature (2-3 eV). Their results showed that the majority (94%) of the CO_2 conversion occurs by reactions (e.g. electron impact dissociation shown in Equation 15) with ground state CO_2 and only 6% by reactions with vibrational excited CO_2 as a considerable fraction of the excited states will eventually de-excite to the ground state of CO_2.[44]

$$e + CO_2 \rightarrow e + CO + O \quad (13)$$

The electron impact dissociation of CO_2 will most likely result in CO in its ground state ($^1\Sigma$) and O atoms in both the ground state (^3P) and metastable state (^1D). However, CO could also be formed in excited states as CO bands are observed in the emission spectra of the CO_2 DBD.[45] The O atoms can react with CO_2 to form CO and O_2 (Equation 16). Oxygen can also be formed from the three-body recombination of atomic oxygen (Equation 17).

$$O + CO_2 \rightarrow CO + O_2 \quad (14)$$

$$O + O + M \rightarrow O_2 + M \quad (15)$$

Increasing the CO_2 flow rate significantly decreases the conversion of CO_2 due to the decrease of the residence time of CO_2 in the discharge zone. In this study, the residence time

362 is decreased by 66.67% from 62.2 s to 20.7 s when the feed flow rate increases from 15
363 $ml \cdot min^{-1}$ to 45 $ml \cdot min^{-1}$ at a discharge length of 120 mm. Significantly decreasing the
364 residence time of CO_2 in the discharge zone results in a reduced chance for CO_2 molecules to
365 react with energetic electrons and reactive species (e.g. O).

366 Figure 4 shows the combined effect of the discharge power and discharge length on CO_2
367 conversion. The maximum CO_2 conversion of 17.3% is achieved at the highest discharge
368 power of 20 W with the discharge length of 150 mm. The discharge length also plays an
369 important role in CO_2 conversion. Increasing the discharge length of the DBD reactor
370 significantly enhances the conversion of CO_2, regardless of the discharge power. This is
371 different to previous results where the variation of discharge length (from 90 mm to 150 mm)
372 only slightly changed the CO_2 conversion in a packed bed DBD reactor.[10] The effect of the
373 discharge length on CO_2 conversion is the result of the two competing effects. In this study,
374 increasing the discharge length from 90 mm to 150 mm leads to the increase of the residence
375 time of CO_2 molecules by 67% (from 23.3 s to 38.9 s) in the discharge region at a constant
376 flow rate of 30 $ml \cdot min^{-1}$, which contributes to the enhancement of CO_2 conversion. On the
377 other hand, a longer discharge length lowers the power density due to the increase of the
378 discharge volume, which results in the decrease of the conversion of CO_2. These results
379 suggest that the change in residence time has a more significant impact on the conversion of
380 CO_2 in our DBD reactor compared to the effects from the reduced power density. In addition,
381 we find the conversion of CO_2 is increased to 18.3% when further increasing the discharge
382 length from 150 mm to 180 mm (outside the range of this design). The interaction of the
383 discharge power and discharge length on the plasma process is considered as insignificant
384 since the contour lines are almost straight. This can also be confirmed by the *p*-value (> 0.05),
385 as listed in Table 3.
386

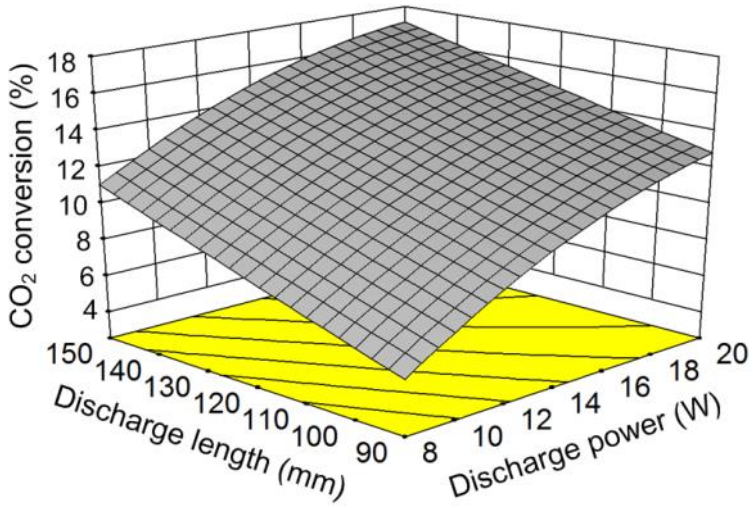

(a)

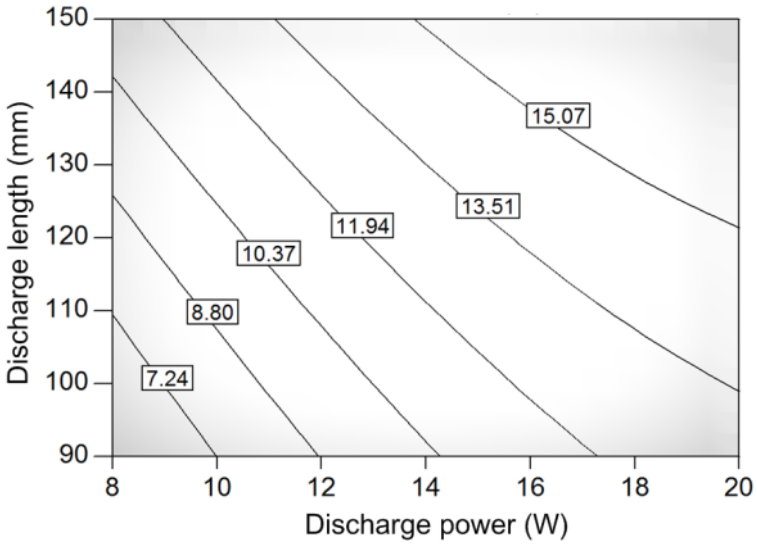

(b)

Figure 4. Effect of discharge power, discharge length and their interaction on CO_2 conversion at a flow rate of 30 ml·min^{-1} (a) 3D surface plot; (b) projected contour plot.

The effects of the discharge length, feed flow rate and their interaction on the conversion of CO_2 are plotted in Figure 5. Similarly, we find the fitted response surface is in the shape of a plane and the contour lines are almost straight. This can also be reflected by a weak variation in the gradient of CO_2 conversion with respect to either the discharge length or the gas flow rate (see Figure 5).The *p*-value of the term related to the interaction of these two parameters is

much higher than the critical value (0.05). These results clearly show that the interaction of the discharge length and gas flow rate on CO_2 conversion is insignificant.

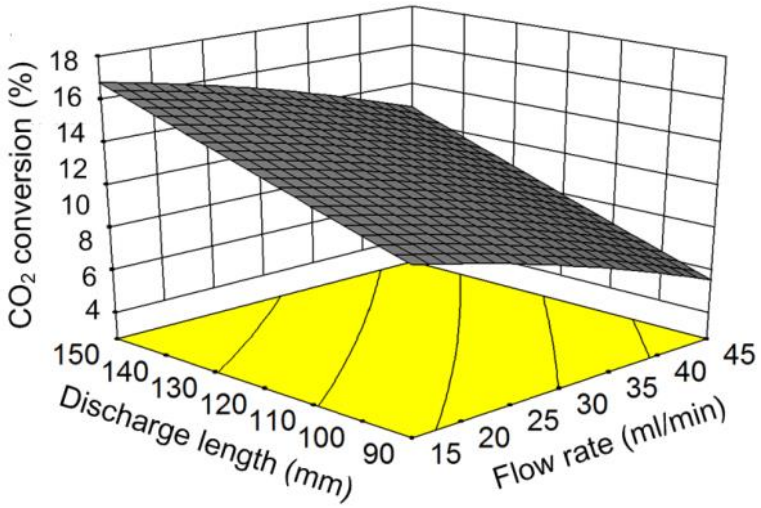

(a)

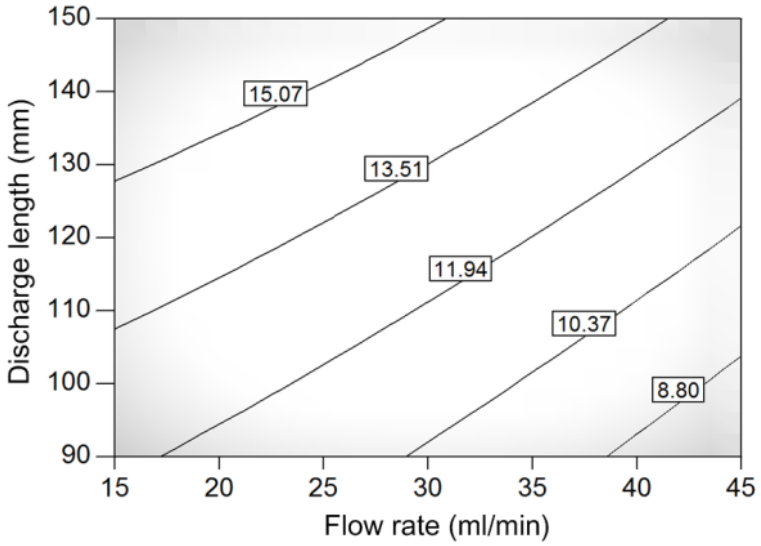

(b)

Figure 5. Effect of CO_2 flow rate, discharge length and their interactions on CO_2 conversion at a discharge power of 14 W (a) 3D surface plot; (b) projected contour plot.

3.3 Effect of process parameters on energy efficiency

The ANOVA results show the effect of the individual process parameters and their interactions on the energy efficiency of the plasma reaction (see Table 4). The terms X_1, X_2, X_3,

412 X_1X_3, X_2X_3, and X_2^2 are identified as the significant factors as their *p*-values are below the
413 critical value of 0.05. The CO_2 flow rate is found to be the most important factor affecting the
414 energy efficiency of the plasma process with the highest *F*-value of 646.16.

415 Figure 6 shows the combined effects of the discharge power and CO_2 feed flow rate on the
416 energy efficiency of the plasma process at a constant discharge length of 120 mm. The
417 maximum energy efficiency of 0.261 mmol·kJ^{-1} is obtained at the lowest discharge power of 8
418 W and highest feed flow rate of 45 ml·min^{-1}. A similar phenomenon was also reported in
419 previous studies, where the highest energy efficiency for the reforming of methane or pure
420 CO_2 decomposition was obtained at lower plasma power and higher reactant flow using either
421 DBD or gliding arc.[27, 31, 40, 45-48] The effect of the discharge power on the energy efficiency
422 shows a similar evolution behaviour when changing the CO_2 flow rate, while the gradient of
423 the energy efficiency with respect to the discharge power is almost constant regardless of the
424 CO_2 flow rate. This suggests the interaction between these two process parameters is very
425 weak in terms of the energy efficiency of the plasma process.

426

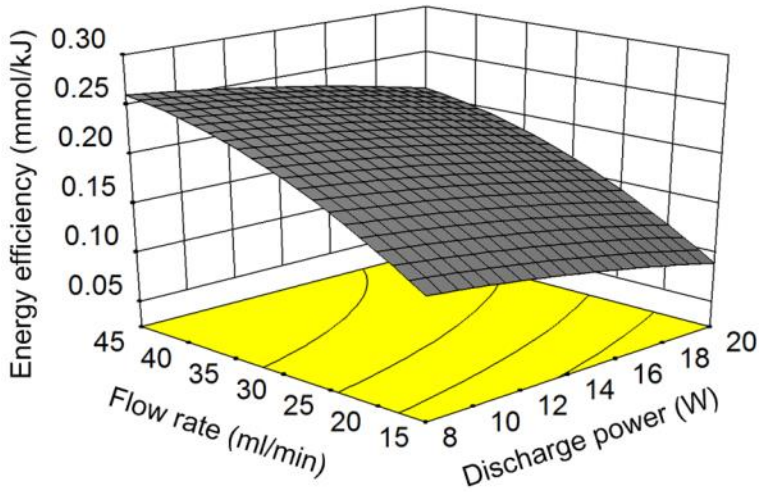

427

428 (a)

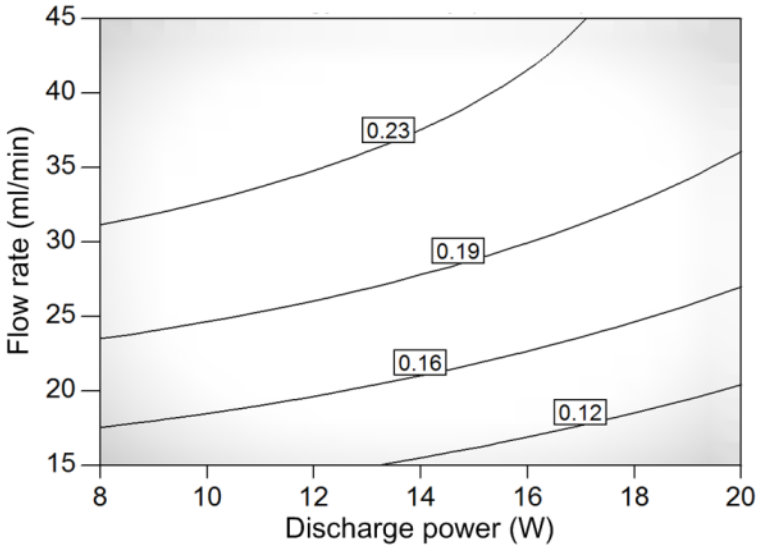

(b)

Figure 6. Effect of discharge power, flow rate and their interaction on the energy efficiency at a discharge length of 120 mm (a) 3D surface plot; (b) projected contour plot.

The interaction of the discharge power and discharge length on the energy efficiency of the plasma CO_2 conversion process is presented in Figure 7. At a constant discharge power and total gas flow rate, increasing the discharge length enhances the conversion of CO_2 due to the increase of the residence time of CO_2 in the plasma zone (Figure 4), which contributes to the enhancement of the energy efficiency of the plasma process. The maximum energy efficiency of the plasma process is achieved at the largest discharge length (150 mm) and lowest discharge power (8 W). At the discharge length of 150 mm, the energy efficiency of the process decreases from 0.293 to 0.193 $mmol \cdot kJ^{-1}$ when the discharge power increases from 8 to 20 W, while the energy efficiency is almost constant with the change of the discharge power at the short discharge length of 90 mm. Similarly, the gradient of the energy efficiency with respect to the discharge length is much higher at a low discharge power (e.g. 8 W) compared to that at a high plasma power (e.g. 20 W). These phenomena demonstrate that there is a significant interaction between the effect of discharge power and discharge length on the energy efficiency of the process, which can also be confirmed by the presence of

contour lines in Figure 7(b). Table 4 also shows that the *p*-value of the term X_1X_3 (< 0.001) is much lower than the level of significance (0.05). Furthermore, the energy efficiency of the plasma process is increased to 0.146 mmol·kJ^{-1} when further increasing the discharge length to 180 mm (outside the range of this design).

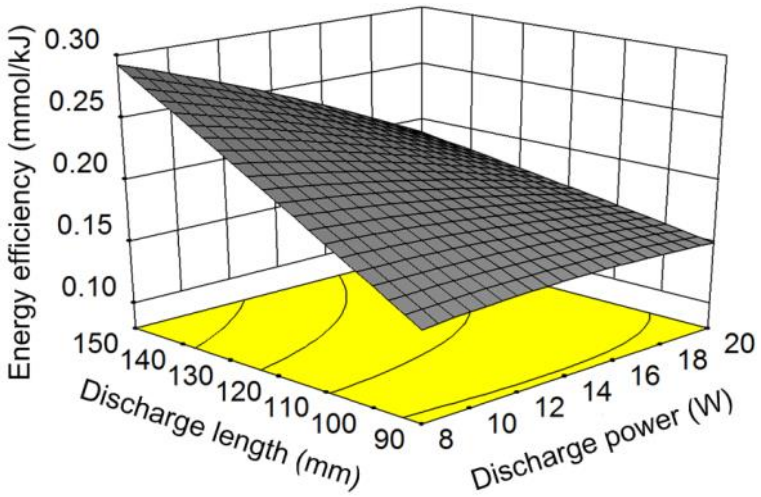

(a)

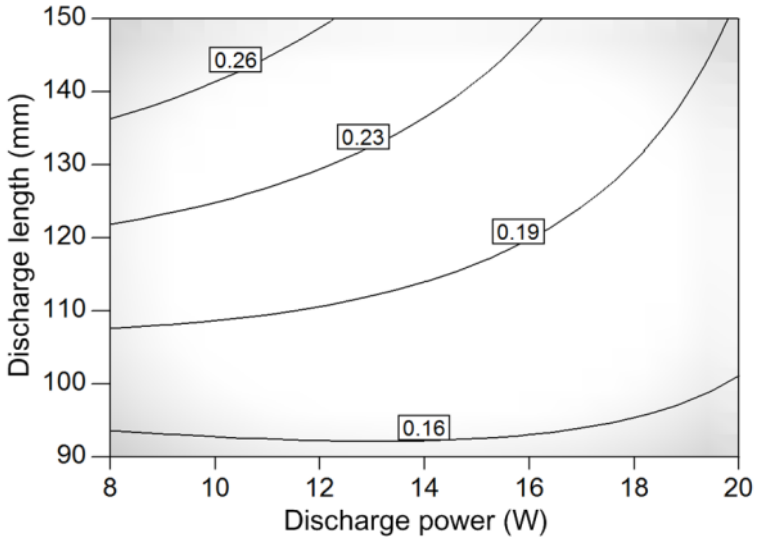

(b)

Figure 7. Effect of discharge power, discharge length and their interaction on the energy efficiency at a flow rate of 30 ml·min^{-1} (a) 3D surface plot; (b) projected contour plot.

Figure 8 shows the combined effects of the gas flow rate and discharge length on the energy efficiency in the plasma CO_2 conversion process. At the shortest discharge length of 90 mm, the energy efficiency of the plasma process increases from 0.1 to 0.171 mmol·kJ^{-1} when the gas flow rate rises from 15 to 35 ml min^{-1}, whereas the energy efficiency is enhanced by over 120% (from 0.138 to 0.310 mmol·kJ^{-1}) with the increase of the gas flow rate at the longest discharge length of 150 mm. This means that the gradient of the energy efficiency with respect to the gas flow rate depends on the discharge length, as plotted in Fig. 8(b). In addition, the energy efficiency decreases significantly when the discharge length changes from 150 mm to 90 mm at the highest CO_2 flow rate of 45 ml·min^{-1}. In contrast, the energy efficiency is almost independent of the discharge length at the lowest flow rate of 15 ml·min^{-1}. These results indicate there is a significant interaction between the effect of discharge length and gas flow rate on the energy efficiency of the plasma process, which can also be confirmed by the low *p*-value (<0.001) of the term X_2X_3 and contour plot.

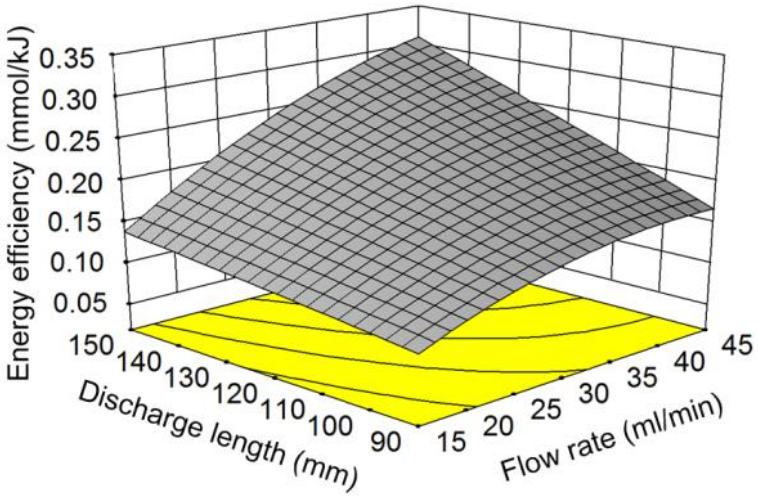

(a)

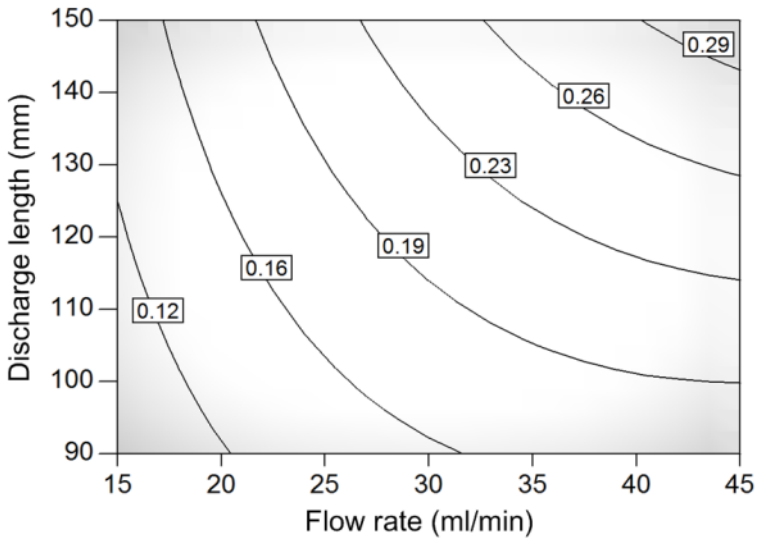

(b)

Figure 8. Effect of flow rate, discharge length and their interaction on the energy efficiency at a discharge power of 14 W (a) 3D surface plot; (b) projected contour plot.

3.4 Process optimization

We find that CO_2 conversion and energy efficiency of the plasma process cannot reach the maximum values simultaneously under the same plasma operating conditions. Increasing the discharge length increases both CO_2 conversion and energy efficiency. However, increasing the discharge power and CO_2 flow rate has an opposite effect on CO_2 conversion and energy efficiency.[40, 49] For example, higher discharge power results in higher CO_2 conversion but lowers the energy efficiency of the process at a fixed CO_2 flow rate, whereas higher reactant flow leads to higher energy efficiency of the plasma process but significantly decreases the conversion of CO_2.

Figure 9 summarizes the CO_2 conversion and energy efficiency of the plasma processing of pure CO_2 using different atmospheric pressure plasma sources. Xu et al. reported a maximum CO_2 conversion of 10.9% in a DC corona discharge reactor at a discharge power of 40 W and a CO_2 flow rate of 30 $ml \cdot min^{-1}$, corresponding to the energy efficiency of 1.68%.[18] They claimed that the highest energy efficiency of 7.28% can be achieved at the expense of very

low CO_2 conversion (3.1%).[18] Paulussen et al. investigated the effect of a wide range of operating parameters (e.g. frequency, discharge power, CO_2 flow rate and inlet gas temperature) on the conversion of CO_2 in a coaxial DBD reactor.[9] They found that the maximum CO_2 conversion of 30 % can be obtained at the lowest CO_2 flow rate of 50 $ml \cdot min^{-1}$ and the highest input power of 200 W. However, the maximum energy efficiency of the plasma process (4.14 %) was not achieved at the same operating conditions, but at the highest CO_2 flow rate of 200 $ml \cdot min^{-1}$.[9] Similarly, Aerts et al. investigated the effect of reactor configurations (e.g., dielectric materials, discharge gap) and operating parameters (e.g., frequency, electrical power and gas flow rate) on the CO_2 decomposition in a DBD reactor.[40] The maximum CO_2 conversion of 34.2% was obtained at an electrical power of 40 W and a gas flow rate of 10 $ml \cdot min^{-1}$, while the maximum energy efficiency (9.25%) was achieved at a lower electrical power (17 W) and a higher gas flow rate (100 $ml \cdot min^{-1}$).[40] Gliding arc discharge has also been used for CO_2 conversion and offers a high flexibility to work in a relatively high reactant gas flow rate and at elevated power levels.[27, 47] A maximum energy efficiency of 19.35% was obtained at a flow rate of 0.86 $l \cdot min^{-1}$, which corresponds to a relatively low CO_2 conversion (15.16%) compared to the maximum CO_2 conversion of 17.3% obtained in their work.[27]

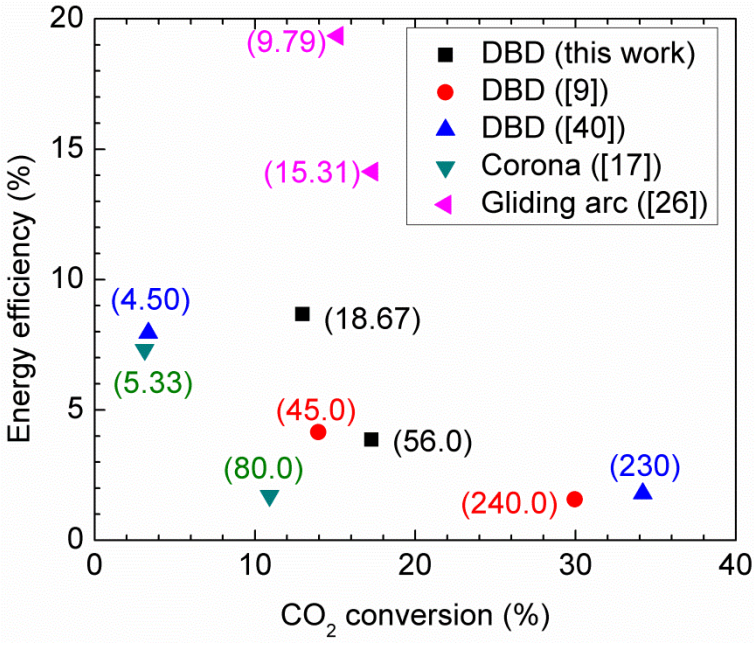

Figure 9. Comparison of CO_2 conversion and energy efficiency in different plasma systems (the number in the brackets is the specific energy density (SED), unit: $kJ \cdot L^{-1}$)

Therefore, a balance between CO_2 conversion and energy efficiency is significantly important for the development of an efficient plasma process for CO_2 conversion. The overall performance of the plasma conversion of CO_2 strongly depends on a wide range of plasma operating conditions. It is essential and indispensable to optimise the plasma CO_2 conversion process with multiple inputs and multiple responses. In this study, the aim of the process optimization is to find a combination of the plasma processing parameters (different factors) that maximize the CO_2 conversion and energy efficiency of the plasma process (different responses) simultaneously. A global desirability function (D) has been introduced as a key parameter to identify the optimal processing parameters and performance in the plasma conversion of CO_2. This function can be calculated from the product of the individual desirability function (d_i) for each response, as shown in the following Equation:[50, 51]

$$D = \left(d_1 \times d_2 \times \ldots \times d_n\right)^{\frac{1}{n}} = \left(\prod_{i=1}^{n} d_i\right)^{\frac{1}{n}} \quad (16)$$

where n is the number of the response in the experiment (n = 2 in this work) and d_i is in the range between 0 (least desirable) and 1 (most desirable). The optimal process and processing parameters can be achieved when the highest value for D is found.

Table 5 shows the different obtained values of global desirability of the plasma process in the process optimization. The optimal process performance - CO_2 conversion (14.2%) and energy efficiency (0.285 mmol·kJ^{-1}, corresponding to 8.0%) for the plasma CO_2 conversion - is achieved at a discharge power of 15.8 W, a feed flow rate of 41.9 ml·min^{-1} and a discharge length of 150 mm as the highest global desirability of 0.816 is obtained. To validate this predicted result, five additional experimental runs are carried out using the optimal process parameters. The results show a fairly good agreement between the experimental results and predicted one with a relative error of less than 5% for both CO_2 conversion and energy efficiency. These reproducible results confirm that DoE can be used to optimize the plasma-assisted CO_2 decomposition process.

Table 5. Process optimization for plasma CO_2 conversion by RSM

Condition	Discharge power (W)	Feed flow rate (ml·min^{-1})	Discharge length (mm)	CO_2 conversion (%)	Energy efficiency (mmol·kJ^{-1})	Global desirability
1	15.8	41.9	150.0	14.3	0.285	0.816
2	16.2	41.4	150.0	14.5	0.280	0.815
3	15.2	39.5	150.0	14.4	0.282	0.814
4	14.7	41.8	150.0	13.8	0.294	0.813
5	15.3	38.2	150.0	14.7	0.275	0.811

4. Conclusion

In this study, the effects of the key plasma process parameters (discharge power, feed flow rate and discharge length) and their interactions on plasma conversion of CO_2 in a coaxial

548 DBD reactor has been investigated through the response surface methodology based on multi-
549 objective optimization. Regression models have been developed to describe the relationships
550 between the plasma process parameters and reaction performance. The significance and
551 adequacy of the models for each response (CO_2 conversion and energy efficiency) have been
552 verified by the analysis of variance. The results show that the conversion of CO_2 increases
553 with increasing discharge power and discharge length, but decreases with the increase of feed
554 flow rate. At a discharge length of 120 mm, the maximum CO_2 conversion of 16.1% is
555 achieved at the highest discharge power of 20 W and lowest CO_2 flow rate of 15 $ml \cdot min^{-1}$.
556 The discharge power is found to be the most important parameter driving the conversion of
557 CO_2, followed by the discharge length and CO_2 flow rate, while the feed flow rate has the
558 most significant effect on the energy efficiency of the process. Increasing the discharge power
559 by changing the applied voltage at a fixed frequency increases the number of microdischarges
560 and average electron density in the CO_2 DBD, both of which contribute to the enhancement of
561 the process performance (e.g. CO_2 conversion). The interactions of different plasma process
562 parameters have a very weak effect on CO_2 conversion. In contrast, there are significant
563 interactions of the discharge length with either discharge power or gas flow rate on the energy
564 efficiency of the plasma process. The optimal CO_2 conversion (14.3%) and energy efficiency
565 (7.98%) for the plasma CO_2 conversion process is achieved at a discharge power of 15.8 W, a
566 feed flow rate of 41.9 $ml \cdot min^{-1}$ and a discharge length of 150 mm, to balance the conversion
567 of CO_2 and energy efficiency of the plasma process. The reproducible experimental results
568 under the theoretical optimal conditions have demonstrated the capability and reliability of the
569 DoE to get a better understanding of the role of the different process parameters and their
570 interactions in the plasma CO_2 conversion reaction for process optimization.
571
572 **Acknowledgements:** Support of this work by the UK EPSRC Grand Challenge CO2Chem
573 Network and Foundation of Key Laboratory of Thermo-Fluid Science and Engineering (Xi'an

574 Jiaotong University), Ministry of Education (China) is gratefully acknowledged. D. H. Mei
575 acknowledges the PhD fellowship co-funded by the Doctoral Training Programme (DTP) of
576 the University of Liverpool and the Chinese Scholarship Council (CSC).

577 Received: ((will be filled in by the editorial staff)); Revised: ((will be filled in by the editorial
578 staff)); Published online: ((please add journal code and manuscript number, e.g., DOI:
579 10.1002/ppap.201100001))

580

581 **Keywords:** CO_2 conversion; design of experiments; dielectric barrier discharge; non-thermal
582 plasma; process optimization
583

584 **References**

585 [1] P. Styring, D. Jansen, H. de Coninck and K. Armstrong, Report *"Carbon Capture and*
586 *Utilisation in the Green Economy: Using CO_2 to Manufacture Fueld, Chemicals and*
587 *Materials,"*Centre for Low Carbon Futures, 2011.

588 [2] Climate Change Act 2008, http://www.legislation.gov.uk/Ukpga/2008/27/Contents
589 (accessed March, 2015).

590 [3] A. Dhakshinamoorthy, S. Navalon, A. Corma, H. Garcia, *Energ. Environ. Sci.* **2012**, *5*,
591 9217.

592 [4] N. S. Spinner, J. A. Vega, W. E. Mustain, *Catal. Sci. Technol.* **2012**, *2*, 19.

593 [5] A. M. Harling, D. J. Glover, J. C. Whitehead, K. Zhang, *Environ. Sci. Technol.* **2008**, *42*,
594 4546.

595 [6] S. Mahammadunnisa, E. L. Reddy, D. Ray, C. Subrahmanyam, J. C. Whitehead, *Int. J.*
596 *Greenh. Gas. Con.* **2013**, *16*, 361.

597 [7] X. Tu, H. J. Gallon, M. V. Twigg, P. A. Gorry, J. C. Whitehead, *J. Phys. D: Appl. Phys.*
598 **2011**, *44*, 274007.

599 [8] M. Ramakers, I. Michielsen, R. Aerts, V. Meynen, A. Bogaerts, Plasma Process. Polym.

2015, 12, 755

[9] S. Paulussen, B. Verheyde, X. Tu, C. De Bie, T. Martens, D. Petrovic, A. Bogaerts, B. Sels, *Plasma Sources Sci. Technol.* **2010**, *19*, 034015.

[10] Q. Q. Yu, M. Kong, T. Liu, J. H. Fei, X. M. Zheng, *Plasma Chem. Plasma Process.* **2012**, *32*, 153.

[11] G. Y. Zheng, J. M. Jiang, Y. P. Wu, R. X. Zhang, H. Q. Hou, *Plasma Chem. Plasma Process.* **2003**, *23*, 59.

[12] T. Kozák, A. Bogaerts, *Plasma Sources Sci. Technol.* **2014**, *23*, 045004.

[13] R. Aerts, R. Snoeckx, A. Bogaerts, *Plasma Process. Polym.* **2014**, *11*, 985

[14] F. Brehmer, S. Welzel, B. L. M. Klarenaar, H. J. van der Meiden, M. C. M. van de Sanden, R. Engeln, *J. Phys. D: Appl. Phys.* **2015**, *48*, 155201.

[15] F. Brehmer, S. Welzel, M. C. M. van de Sanden, R. Engeln, *J. Appl. Phys.* **2014**, *116*, 123303.

[16] D. H. Mei, X. B. Zhu, Y. L. He, J. D. Yan, X. Tu, *Plasma Sources Sci. Technol.* **2015**, *24*, 015011.

[17] T. Mikoviny, M. Kocan, S. Matejcik, N. J. Mason, J. D. Skalny, *J. Phys. D: Appl. Phys.* **2004**, *37*, 64.

[18] W. Xu, M. W. Li, G. H. Xu, Y. L. Tian, *Jpn. J. Appl. Phys.* **2004**, *43*, 8310.

[19] G. Horvath, J. D. Skalny, N. J. Mason, *J. Phys. D: Appl. Phys.* **2008**, *41*, 225207.

[20] A. Yamamoto, S. Mori, M. Suzuki, *Thin Solid Films* **2007**, *515*, 4296.

[21] J. Y. Wang, G. G. Xia, A. M. Huang, S. L. Suib, Y. Hayashi, H. Matsumoto, *J. Catal.* **1999**, *185*, 152.

[22] L. F. Spencer, A. D. Gallimore, *Plasma Sources Sci. Technol.* **2013**, *22*, 015019.

[23] A. Vesel, M. Mozetic, A. Drenik, M. Balat-Pichelin, *Chem. Phys.* **2011**, *382*, 127.

[24] M. Tsuji, T. Tanoue, K. Nakano, Y. Nishimura, *Chem. Lett.* **2001**, 22.

[25] L. T. Hsieh, W. J. Lee, C. T. Li, C. Y. Chen, Y. F. Wang, M. B. Chang, *J. Chem. Technol.*

626 *Biotechnol.* **1998**, *73*, 432.

627 [26] L. F. Spencer, A. D. Gallimore, *Plasma Chem. Plasma Process.* **2011**, *31*, 79.

628 [27] A. Indarto, D. R. Yang, J. W. Choi, H. Lee, H. K. Song, *J. Hazard. Mater.* **2007**, *146*,

629 309.

630 [28] T. Nunnally, K. Gutsol, A. Rabinovich, A. Fridman, A. Gutsol, A. Kemoun, *J. Phys. D*

631 *Appl. Phys.* **2011**, *44*, 274009.

632 [29] S. L. Brock, M. Marquez, S. L. Suib, Y. Hayashi, H. Matsumoto, *J. Catal.* **1998**, *180*,

633 225.

634 [30] S. L. Brock, T. Shimojo, M. Marquez, C. Marun, S. L. Suib, H. Matsumoto, Y. Hayashi,

635 *J. Catal.* **1999**, *184*, 123.

636 [31] R. Snoeckx, Y. X. Zeng, X. Tu, A. Bogaerts, *RSC Adv.* **2015**, *5*, 29799.

637 [32] C. De Bie, B. Verheyde, T. Martens, J. van Dijk, S. Paulussen, A. Bogaerts, *Plasma*

638 *Process. Polym.* **2011**, *8*, 1033.

639 [33] C. De Bie, J. van Dijk, A. Bogaerts, *J. Phys. Chem. C* **2015**, in press.

640 [34] R. Snoeckx, R. Aerts, X. Tu, A. Bogaerts, *J. Phys. Chem. C* **2013**, *117*, 4957.

641 [35] D. C. Montgomery, *Design and Analysis of Experiments*, Wiley, New York, **2012.**

642 [36] L. Wu, K. L. Yick, S. P. Ng, J. Yip, *Expert. Syst. Appl.* **2012**, *39*, 8059.

643 [37] K. S. Prasad, C. S. Rao, D. N. Rao, *J. Braz. Soc. Mech. Sci.* **2012**, *34*, 75.

644 [38] H. Ebrahimi-Najafabadi, R. Leardi, M. Jalali-Heravi, *J Aoac Int* **2014**, *97*, 3.

645 [39] C. S. Ramachandran, V. Balasubramanian, P. V. Ananthapadmanabhan, *J. Therm. Spray.*

646 *Technol.* **2011**, *20*, 590.

647 [40] R. Aerts, W. Somers, A. Bogaerts, *ChemSusChem* **2015**, *8*, 702.

648 [41] X. Tu, B. Verheyde, S. Corthals, S. Paulussen, B. F. Sels, *Phys. Plasmas* **2011**, *18*,

649 080702.

650 [42] L. F. Dong, X. C. Li, Z. Q. Yin, S. F. Qian, J. T. Ouyang, L. Wang, *Chinese Phys. Lett.*

651 **2001**, *18*, 1380.

[43] A. Fridman, *Plasma Chemistry*, Cambridge University Press, New York, **2008.**

[44] R. Aerts, T. Martens, A. Bogaerts, *J Phys Chem C* **2012**, *116*, 23257.

[45] X. Tu, J. C. Whitehead, *Appl. Catal. B-Environ.* **2012**, *125*, 439.

[46] S. Y. Liu, D. H. Mei, Z. Shen, X. Tu, *J. Phys. Chem. C* **2014**, *118*, 10686.

[47] X. Tu, J. C. Whitehead, *Int. J. Hydrogen Energ.* **2014**, *39*, 9658.

[48] X. Duan, Y. Li, W. Ge, B. Wang, *Greenhouse Gas Sci Technol.* **2015**, *5*, 131.

[49] A. Lebouvier, S. A. Iwarere, P. d'Argenlieu, D. Ramjugernath, L. Fulcheri, *Energ. Fuel.* **2013**, *27*, 2712.

[50] G. Derringer, R. Suich, *J. Qual. Technol.* **1980**, *12*, 214.

[51] N. R. Costa, J. Lourenco, Z. L. Pereira, *Chemometr. Intell. Lab.* **2011**, *107*, 234.

Table of contents

Optimization of CO_2 conversion in a cylindrical dielectric barrier discharge reactor using design of experiments

Danhua Mei, Ya-Ling He, Shiyun Liu, Joseph Yan, Xin Tu*

Design of Experiments has been used to optimize the plasma conversion of CO_2 into CO and oxygen in a dielectric barrier discharge reactor. The importance of different independent process parameters, especially the interactions of these parameters on the plasma conversion of CO_2 has been investigated.